

Measurement of the effective focal shift in an optical trap

Keir C. Neuman,* Elio A. Abbondanzieri, and Steven M. Block

Departments of Biological Sciences and Applied Physics, Stanford University, Stanford, California 94305-5020

Received November 3, 2005

The focus of an oil-immersion microscope objective is shifted because of the refractive-index mismatch between the cover glass and the aqueous sample. We present a procedure with which to determine the focal shift by use of an inverted microscope equipped with optical tweezers. As the position of the sample chamber is scanned vertically, we measure the axial displacement of an optically trapped bead; the relative motion of the bead with respect to the surface supplies the effective focal shift. Measurements of this quantity deviate from electromagnetic calculations of the focal shift, a discrepancy attributable to the depth-dependent decrease in axial trap stiffness that arises from spherical aberration. © 2005 Optical Society of America

OCIS codes: 120.1880, 120.3180.

Focusing light through an interface between mismatched refractive indices results in a displacement of the focal position relative to its location in a uniform medium. The origin of this shift is readily conveyed by a geometrical picture [Fig. 1(a)]. As light from a medium of higher refractive index is focused into a medium of lower index, converging rays bend away from the surface normal, displacing the focus toward the interface. However, this ray-optic representation fails to supply the correct magnitude of the focal shift for objective lenses with high numerical aperture (NA), where the paraxial ray approximation breaks down. More comprehensive theoretical treatments that incorporate diffraction at the interface have been developed¹; from these, the theoretical focal shift can be computed with improved precision. Several experimental estimates of the focal shift have been carried out; these have been used primarily to correct three-dimensional data sets collected from confocal microscopes.^{2,3} In the latter case, the focal shift is typically computed from the ratio of the apparent thickness of a small fluorescent object to its known thickness.

Accurate determinations of axial position are important in optical trapping applications as well, for which one needs to know the value of the focal shift to compute the true displacement of an object generated by raising or lowering the microscope objective—or, equivalently, by raising or lowering the sample chamber. In an optical trap it is not the axial position of the focal spot *per se* but the axial position of the trapped object that is sought. Here we define the ratio of axial bead displacement to cover-glass displacement as the effective focal shift, to distinguish it from the shift of the optical focus.

We present a practical, precise method for determining the effective focal shift associated with focusing a laser with a high-NA objective in an optical trapping instrument. Our approach relies on detecting the small oscillations produced by interference between forward-scattered light and light reflected between the trapped bead and the planar cover glass surface [Fig. 1(b), inset]. As the cover glass (or the objective) is displaced axially, the changing separation between the bead and the surface modulates the in-

terference pattern. This signal provides a sensitive measure of the distance between bead and cover glass. Employing this approach, we measured the value of the effective focal shift over a range of refractive-index mismatches and compared our results with theory.

Individual, 500-nm-diameter polystyrene beads were suspended in a mixture of water and glycerol and optically trapped by a Nd:YLF ($\lambda = 1047$ nm) or a Nd:YVO₄ ($\lambda = 1064$ nm) infrared laser.^{4,5} A quadrant

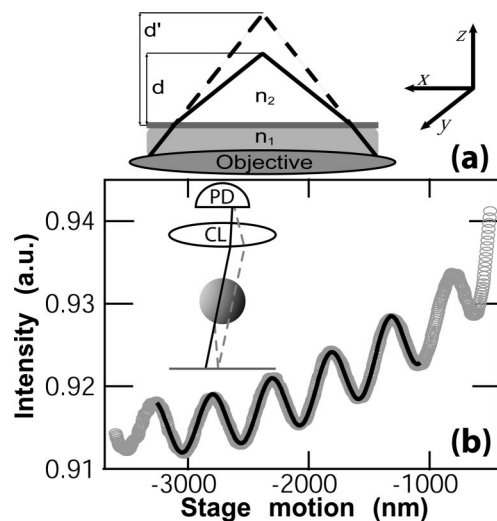


Fig. 1. (a) Origin of the focal shift. Convergent light crosses the interface between n_1 and n_2 ($n_1 > n_2$) and comes to a focus at position d rather than d' , where the focus would occur in the absence of an index mismatch. The coordinate system defines the axes. Light propagates in the z direction. The immersion oil (lighter shading) and the cover glass (thick horizontal line) that form the bottom of the sample chamber have index n_1 ; the aqueous fluid in the chamber has index n_2 . (b) Axial position-dependent interference signal. The intensity of the forward-scattered light from a trapped bead is measured by a photodetector (PD, inset) located in a plane optically conjugate to the condenser back focal plane (CL, inset). As the stage is moved, the interference between the direct light (inset, darker curve) and the reflected light (inset, lighter, dashed curve) produces a periodic intensity modulation (lighter circles) that can be fitted by a sinusoidal function (darker curve).

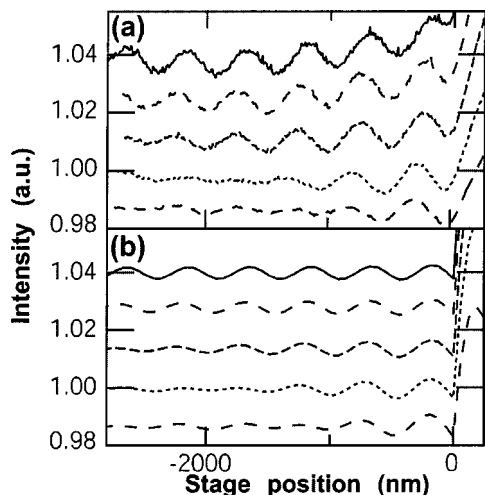


Fig. 2. (a) Dependence of interference signal on NA. The photodetector voltage was measured as a trapped bead and was moved relative to the cover glass for a series of decreasing iris aperture stops on the condenser; traces are arranged in order of decreasing NA from bottom to top and are displaced on the ordinate for clarity. (b) Computed position signals for collection NA estimated from the traces in (a). From bottom to top, the NA values are 1.16, 1.03, 0.71, 0.54, and 0.26.

photodiode placed in the back focal plane measured the light scattered by the bead.^{5,6} The normalized sum signal from the quadrant photodiode was measured as the position of the stage was scanned in the axial direction [Fig. 1(b)]. To confirm that the observed intensity modulation was due to reflections between the bead and the glass-medium interface, we compared the measured curves for different detector NAs with theoretical predictions (Fig. 2). The focused laser beam was modeled with beam-shape coefficients derived from the localized approximation to an on-axis Davis first-order beam, as described by Lock and Gouesbet [Ref. 7, Eq. (59)]. These coefficients were derived from a Gaussian beam, but they describe a field that satisfies Maxwell's equations exactly and is well behaved over all space. The scattering from a sphere located near a planar surface was solved by use of an extension of Mie theory.⁸ The interference of the scattered and unscattered fields was calculated in the far field and used to approximate the signal obtained at the back focal plane of the condenser.⁹ Qualitatively, the observed and calculated intensity modulations show good agreement, supporting the notion that multiple reflections from the bead-cover-glass system represent the source of interference. As anticipated, the periodicity of this interference was independent of the size and composition of the bead, which acts only as a partially reflective surface in this system. Additional measurements were performed with a different apparatus that used a high-power laser at 1064 nm for trapping and a secondary, low-power laser at 830 nm to detect the bead's position. Here the observed signal periodicity corresponded to 830 nm, confirming that the modulation is due to the interference mechanism described rather than to a periodic change in the trapping potential.

Paraxial rays tend to remain in phase for large bead-cover-glass separations, whereas rays scattered at higher angles describe longer, more-disperse paths in reflecting off the cover glass. Therefore, as the NA of the condenser was decreased, the intensity modulation became more regular and persisted over greater distances (Fig. 2); for this reason, measurements of the effective focal shift were performed at the lowest practical NA.

The interference of light reflected between the bead and the cover glass can be modeled as a Fabry-Perot interferometer. The finesse of the bead-cover-glass system at the lowest detection NA measured ~ 0.009 , which is comparable to the calculated value, ~ 0.02 . The intensity of light transmitted through to the detector can therefore be approximated by $A + B \cos(4\pi nd/\lambda_0)$, where n is the refractive index of the medium, d is the bead-cover-glass separation, and λ_0 is the vacuum wavelength. We acquired interference traces by moving the stage approximately $3\text{--}4\ \mu\text{m}$ axially while we recorded the light's intensity. We determined the spatial frequency by fitting the intensity-stage position relationship to a function of the form $P_l(z) + P_m(z)\cos(\Omega z + \varphi)$, where $P_l(z)$ and $P_m(z)$ are polynomials of orders l and m , respectively, Ω is the spatial frequency, φ is a constant phase term, and z is the stage position [Fig. 1(b)]. Polynomial functions of order 2 or 3 were sufficient to yield accurately the spatial frequency Ω that represents the parameter of interest. The effective focal shift is then given by Ω/Ω_0 , the ratio of this frequency to the spatial frequency in the absence of a focal shift, $\Omega_0 = 4\pi n/\lambda_0$.

The theoretical focal shift can be derived from a calculation of the axial distribution of the electric field for plane-polarized light focused through an interface of mismatched indices, as solved by Wiersma *et al.* [Ref. 1, Eq. (10)]. The position of the focus relative to the interface was solved numerically for a range of interface positions. For displacements up to $\sim 10\ \mu\text{m}$, the position of the focus is linearly related to the interface position with a slope equal to the focal shift. Calculations were performed based on a NA of 1.3 and refractive index $n = 1.515$, appropriate for both the immersion oil and the cover glass. The index of the trapping medium was computed from a weighted average of the refractive indices of water (1.33) and glycerol (1.45).

Experimental and theoretical focal-shift data for a range of refractive-index mismatches are compared in Fig. 3. Focal shifts measured at wavelengths of 1.064 and 1.047 μm were statistically indistinguishable. The experimental measurements deviate from the calculated focal shift when the mismatch is large but agree for smaller values.

The observed difference between the effective focal shift and its calculated value is explained by a small displacement of the equilibrium trapping position as the separation between the bead and the cover glass increases. The axial stiffness generated by the focal gradient tends to degrade with increasing depth of focus, causing the equilibrium trapping position to move downbeam from the focal point. To confirm that

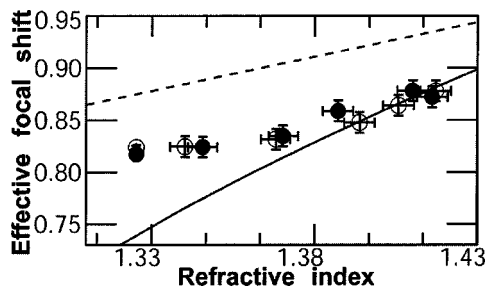


Fig. 3. Measured and calculated focal shift versus refractive index of the second medium. The effective focal shift was measured for both 1.064- μm (open circles) and 1.047- μm (filled circles) wavelengths. The refractive index of the first medium was 1.515 (immersion oil and cover glass). We varied the index of the second medium by mixing water and glycerol. The calculated focal shift (solid curve) was determined at 1.064 μm as described in the text and is indistinguishable from the shift at 1.047 μm . The focal shift calculated in the paraxial limit (n_2/n_1 ; dashed curve) is included for comparison.

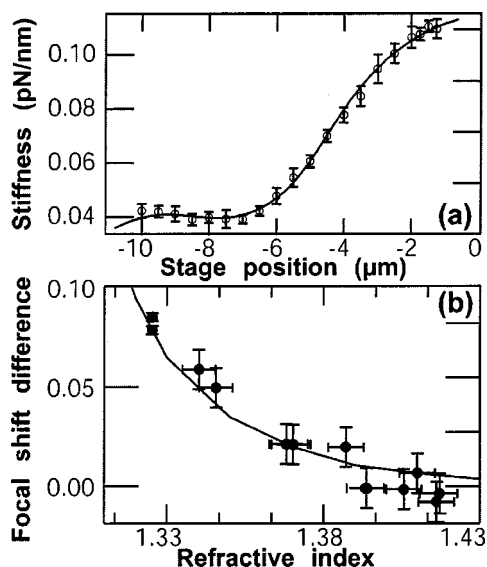


Fig. 4. (a) Comparison of measured (open circles) and estimated (solid curve) axial trap stiffness versus stage position for a bead trapped in water. The stage position was measured relative to the point where the focus lies at the glass–water interface. The curve plots the second derivative of the axial intensity from theory (see text), rescaled. (b) Difference between calculated and measured focal shift versus index of the second medium (filled circles), compared with a model in which this difference is approximated by the depth-dependent drop in axial stiffness (solid curve). The rates of change of stiffness with depth were calculated for various indices as in (a); then each rate was fitted to a line over the relevant region of measurement (1–3.5 μm). These slopes were then rescaled and plotted as shown.

this phenomenon accounts for our observations, we determined the axial stiffness as a function of stage position for a trapped bead in water, using the roll-off frequency of the power spectrum,⁵ which supplies the

ratio of the stiffness to the damping. We then compared this depth-dependent stiffness with a simplified model in which the stiffness is approximated by the second derivative of the calculated axial intensity [Fig. 4(a)]. Up to a scaling factor and offset term, the measured and calculated curves agree well. The difference between the measured focal shift and the calculated value (based on Ref. 1) as a function of index mismatch is shown in Fig. 4(b). We compared these values with a theoretical estimate that we derive by assuming that the difference is due to the diminution of trap stiffness with depth. Once again, up to an arbitrary scaling factor, the discrepancy is well described by the model. As the mismatch decreases (i.e., for greater values of the second index), so does the degree of spherical aberration that is responsible for the drop in axial stiffness; this accounts for the agreement between the measured and the calculated focal shifts at large values of the index of the second medium. Whereas such a simplified theory does not permit a fully quantitative analysis, it correctly predicts the trend of the data and is consistent with previous measurements.^{10,11}

Our findings underscore the importance of measuring this effective focal shift directly rather than simply computing it from theory or relying on focal-shift parameters determined by other means. Owing to the depth-dependent decrease in axial stiffness associated with spherical aberration, these other methods will tend to overestimate the focal shift obtained in practice, particularly for large index mismatches. By using the method described here it is possible to determine true axial displacements in an optical trap with nanometer-level precision.

S. M. Block's e-mail address is sblock@stanford.edu.

*Present address, Laboratoire de Physique Statistique, École Normale Supérieure, Paris 75005, France.

References

1. S. H. Wiersma, P. Torok, T. D. Visser, and P. Varga, *J. Opt. Soc. Am. A* **14**, 1482 (1997).
2. N. S. White, R. J. Errington, M. D. Fricker, and J. L. Wood, *J. Microsc.* **181**, 99 (1996).
3. S. Hell, G. Reiner, C. Cremer, and E. H. K. Stelzer, *J. Microsc.* **169**, 391 (1993).
4. K. C. Neuman, E. A. Abbondanzieri, R. Landick, J. Gelles, and S. M. Block, *Cell* **115**, 437 (2003).
5. K. C. Neuman and S. M. Block, *Rev. Sci. Instrum.* **75**, 2787 (2004).
6. K. Visscher, S. P. Gross, and S. M. Block, *IEEE J. Sel. Top. Quantum Electron.* **2**, 1066 (1996).
7. J. A. Lock and G. Gouesbet, *J. Opt. Soc. Am. A* **11**, 2503 (1994).
8. G. Videen, *J. Opt. Soc. Am. A* **8**, 483 (1991).
9. F. Gittes and C. F. Schmidt, *Opt. Lett.* **23**, 7 (1998).
10. E. Fallman and O. Axner, *Appl. Opt.* **42**, 3915 (2003).
11. K. B. Kim, H. I. Kim, I. J. Joo, C. H. Oh, S. H. Song, P. S. Kim, and B. O. Park, *Opt. Commun.* **226**, 25 (2003).